

Ground Penetrating Radar  
The first peer-reviewed scientific journal dedicated to GPR

## A PRACTICAL GUIDE ON USING SPOT-GPR, A FREWARE TOOL IMPLEMENTING A SAP-DoA TECHNIQUE

SIMONE MESCHINO<sup>1</sup> & LARA PAJEWSKI<sup>2</sup>

<sup>1</sup> AIRBUS DS, SAR SYSTEMS ENGINEERING, FRIEDRICHSHAFEN, GERMANY  
SIMONE.MESCHINO@GMAIL.COM

<sup>2</sup> SAPIENZA UNIVERSITY OF ROME, DEPARTMENT OF INFORMATION ENGINEERING,  
ELECTRONICS AND TELECOMMUNICATIONS, ROME, ITALY  
LARA.PAJEWSKI@UNIROMA1.IT

### ABSTRACT

*This is a software paper, which main objective is to provide practical information on how to use SPOT-GPR release 1.0, a MATLAB®-based software for the analysis of ground penetrating radar (GPR) profiles. The software allows detecting targets and estimating their position in a two-dimensional scenario, it has a graphical user interface and implements an innovative sub-array processing method. SPOT-GPR was developed in the framework of the COST Action TU1208 “Civil Engineering Applications of Ground Penetrating Radar” and is available for free download on the website of the Action ([www.GPRadar.eu](http://www.GPRadar.eu)).*

**KEYWORDS:** Ground Penetrating Radar; Detection and localization of buried structures; Sub-array processing; Direction of arrival algorithms; Matched filter technique.

### 1. INTRODUCTION

SPOT-GPR [1] stands for “Sub-array Processing Open Tool for GPR applications” and is a MATLAB®-based software for the analysis of ground penetrating radar (GPR) profiles, with the main purposes of detecting and localizing targets. The tool comes with a graphical user interface (GUI) and implements an innovative sub-array processing (SAP) method, which exploits smart-antenna and radar algorithms. SPOT-GPR was developed during three Short-Term Scientific Missions (STSMs) funded by European Cooperation in Science and Technology (COST, [www.cost.eu](http://www.cost.eu)) and carried out in the framework of the COST Action TU1208 “Civil Engineering Applications of Ground Penetrating Radar.” The software is available for free download on the website of the Action ([www.GPRadar.eu](http://www.GPRadar.eu)).

The input of the software is a GPR profile (otherwise called ‘B-scan’ or ‘radargram’ by the GPR community). This is partitioned in sub-radargrams, with just a few traces (‘A-scans’) per sub-radargram. The multi-frequency information enclosed in each trace is exploited and a dominant direction of arrival (DoA) [2] of the electromagnetic field is calculated for every sub-radargram. All the estimated DoAs are triangulated and a pattern of crossings is obtained, which is more densely populated around target locations. Such pattern is filtered, in order to remove a noisy background of unwanted crossings, and is then processed by applying a statistical procedure. Finally, the number of targets and their positions are predicted. For DoA estimation, SPOT-GPR uses the MULTiple Signal Classification (MUSIC) [3] algorithm, in combination with the matched filter technique [4]. A description of the method implemented in SPOT-GPR, including detailed information about its advantages and limits, is found in [1].

SPOT-GPR was successfully tested on GPR synthetic radargrams, generated by using the open-source finite-difference time-domain simulator *gprMax* [5] ([www.gprmax.com](http://www.gprmax.com)). Moreover, it was compared with MATLAB® codes implementing two different methods, with good results: a classical hyperbola analysis based on a minimum mean square error technique [6] (see [1]), and an advanced algorithm for the localization of hyperbola apexes and characteristic points based on artificial neural networks and pattern recognition [7-9] (this comparison is not yet published at the time when this paper is written).

The present paper aims to provide practical information on how to use SPOT-GPR and includes some examples. It is advised to read [1] before reading the following sections of this paper and using the software.

## 2. DESCRIPTION OF THE SOFTWARE

As mentioned in the introduction, SPOT-GPR needs to receive a radargram as main data input, i.e., a set of N traces. The software gives the following output:

1. A plot of the radargram.
2. A plot of the compressed Fast Fourier Transform (FFT) of the radargram, over the signal bandwidth, showing the compressed frequency-content of the field measured by the GPR.

3. An interactive “crossing pattern” that allows the user estimating the number of targets and their coordinates in a two-dimensional scenario (horizontal position and burial depth).

The approach implemented in SPOT-GPR is schematized in Figure 1.

In the field of smart antennas, DoA techniques are used to estimate the number of incident signals impinging over an antenna array, along with their arrival directions. A SAP approach is adopted for the DoA-based detection of electromagnetic sources lying in the near field of an antenna array. In particular, the array of  $N$  receivers is partitioned in  $M$  sub-arrays, so that the sources can be assumed to be locally planar at each sub-array. Then, by applying DoA estimation algorithms, it is possible to predict the dominant direction of the incoming signal at each sub-array. By triangulating all the DoAs estimated by the sub-arrays, a pattern of crossings can be obtained. This pattern can be filtered in order to remove a noisy background of unwanted crossings and a subset of crossings  $\{x,y\}_k$  can be extracted, with  $k = 1, \dots, K$ , where  $K$  is the number of crossings. Subsequently, the number of sources and their positions can be estimated, by averaging the coordinates of clustered crossings.

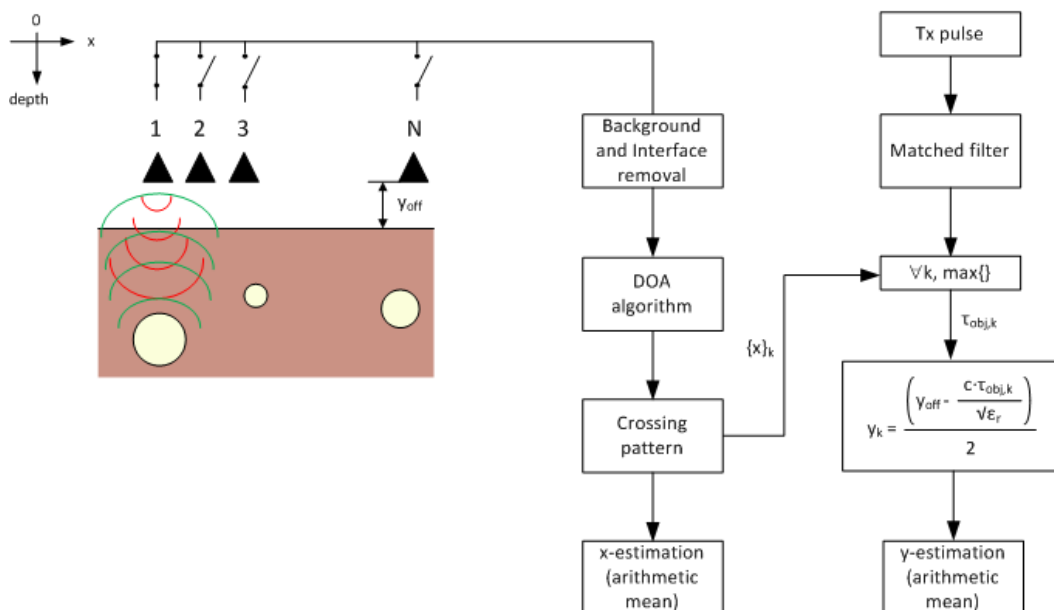


**FIG. 1** – Geometry of the GPR scenario and signal-processing block diagram, illustrating the method implemented in SPOT-GPR.

In the scenario that we considered (namely, the use of a SAP-DoA approach for the interpretation of GPR radargrams acquired over a soil or structure), the situation is similar. The electromagnetic sources are the currents induced on the sought targets and DoA algorithms can provide information about where the electromagnetic field back-scattered by the targets comes from.

In order to work in near-field conditions, the radargram to be analysed has to be partitioned in sub-radargrams of suitable size (SAP approach); then, a dominant DoA is predicted for each sub-radargram. The estimated angles are triangulated, thus obtaining a set of crossings with intersections condensed around object locations. This pattern is filtered, in order to remove the unwanted crossings and according to the desired false-alarm rate. The horizontal coordinates of the crossings,  $\{x\}_k$ , are processed by using a SAP-DoA approach without pulse compression. For each  $x_k$ , the nearest A-scan is then compressed in the time domain, by exploiting information about the pulse emitted by the GPR. Afterwards, the time instant value corresponding to the maximum of the pulse-compressed signal  $\tau_{obj,k}$  is extracted and the y-coordinate (depth) is estimated for the k-th crossing. When all the crossings of the pattern have been processed, the (x,y) position of each target is calculated by a simple coordinate average.

The SPOT-GPR archive, downloadable from the TU1208 website, includes the files listed and described in Table 1. Moreover, the package includes a folder called “input” where some datasets are stored: they can be used to familiarize with the software.

The layout of the GUI, before executing the software, is shown in Fig. 2(a). It includes three main sections, corresponding to three steps to be done by the user in order to obtain the estimation of target positions:

Step-1. **Load input files:** the user is required to select the relevant input files (background, simulation, Tx-pulse). More details about the content of such files and required format are given in Subsection 2.1.

Step-2. **Settings:** the user is required to encode the simulation settings, as described in Subsection 2.2.

Step-3. **Spotting:** by interactively drag the mouse on the spotting figure, the user will extract the estimated positions of the targets,

calculated by the software from the coordinates of the crossings included within the selected area, as described in Subsection 2.3.

The three steps of the procedure have to be performed consecutively and in the order that we outlined.

**TABLE 1 – SPOT-GPR PACKAGE FILES.**

<b>DESCRIPTION</b>	<b>INPUT</b>	<b>OUTPUT</b>
<i>File Name: COST_DOA_main.fig</i>		
<i>GUI main figure, used by the GUI main code</i>	<i>None</i>	<i>None</i>
<i>File Name: COST_DOA_main.m</i>		
<i>GUI main code</i>	<i>None</i>	<i>None</i>
<i>File Name: COST_DOA_init_status_flag.m</i>		
<i>Function for the initialization of variables</i>	<i>None</i>	<i>None</i>
<i>File Name: COST_DOA_bscan2D.m</i>		
<i>B-scan plot function</i>	<i>B-Scan data</i>	<i>B-scan plot</i>
<i>File Name: COST_DOA_fft.m</i>		
<i>B-scan FFT calculation and plot function</i>	<i>Electric-field values, interpolation factor</i>	<i>FFT plot</i>
<i>File Name: COST_DOA_sel.m</i>		
<i>SAP-DoA evaluation for each sub-array</i>	<i>Angular scan resolution, number of sub-arrays, number of elements per sub-array, steering vector, correlation matrix</i>	<i>DoA vector for each preferred DoA method (only MUSIC is implemented in release 1.0)</i>
<i>File Name: COST_DOA_code.m</i>		
<i>Function that builds the SAP-DoA crossing pattern, by triangulating DoAs, and filters the noise</i>	<i>None - For release 1.0 the input parameters of this function are freezed and not editable in the GUI</i>	<i>x-y coordinates of the crossings composing the refined crossing pattern</i>
<i>File Name: COST_DOA_cross_centre_estim.m</i>		
<i>Target localization function</i>	<i>Rectangular area containing crossings to be considered (dragged by user)</i>	<i>Target position estimation</i>
<i>File Name: logo_COST.png</i>		
<i>COST logo</i>	<i>None</i>	<i>None</i>

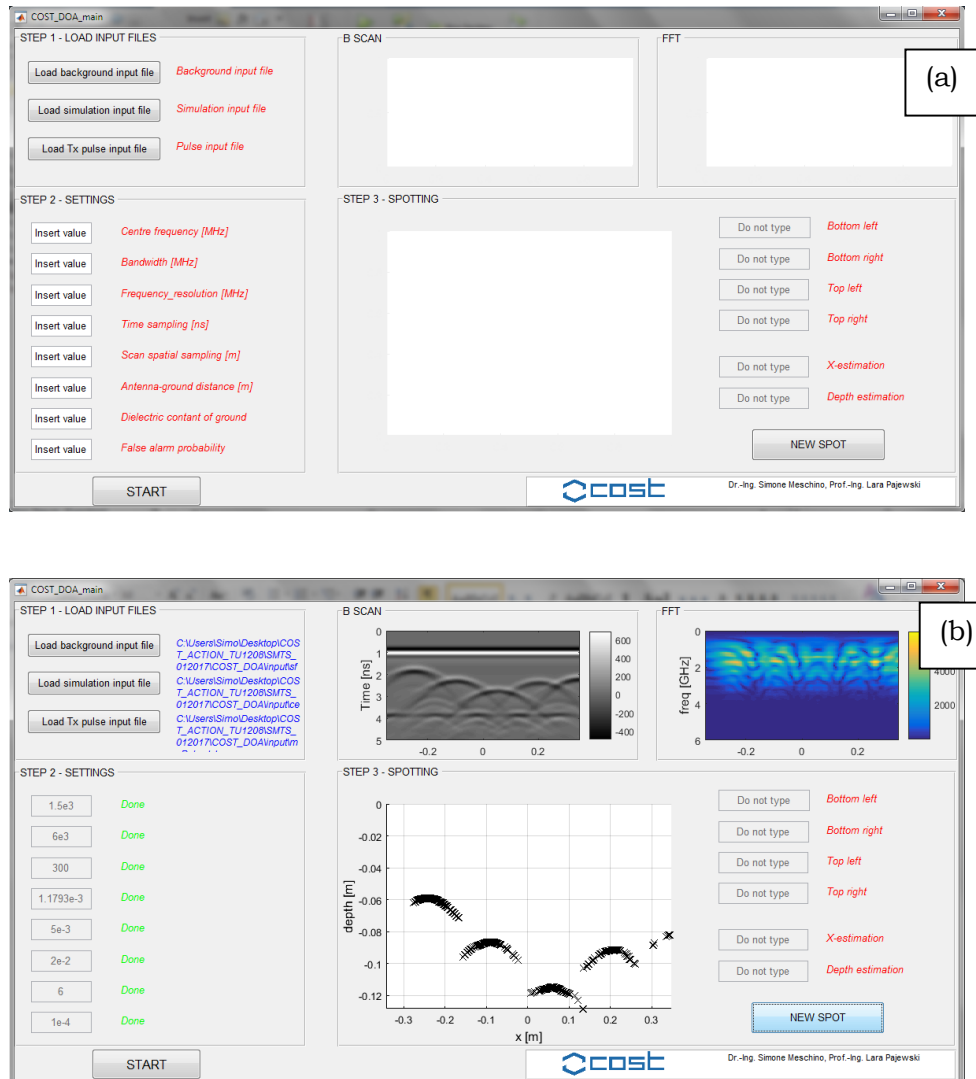


**FIG. 2** – Layout of the COST\_DoA GUI (release 1.0) (a) before and (b) after executing the software.

The layout of the GUI after executing the software is shown in Figure 2(b) and consists of:

- A grey-scale map of the synthetic or experimental radargram.
- A colour map of the FFT of the compressed radargram.
- The spotting interactive panel, where the user can select an area by simply dragging a rectangular region with the mouse. The relevant estimation of the target position is provided by the software in the dedicated box, on the right.

## 2.1. STEP 1: LOAD INPUT FILES

The “Step 1: LOAD INPUT FILES” panel is shown in Figure 3. Initially, each loading button is accompanied by a short description of the required file, in red. Such description disappears when the file is selected (and is replaced by the file path, in blue). Three files are required:

- Background input file (electric field amplitude measured by the GPR in the absence of the targets).
- Simulation input file (radargram).
- Tx-pulse input file (pulse emitted by the GPR).

The input files have to be formatted as described hereafter, and have to be saved as .txt text files.

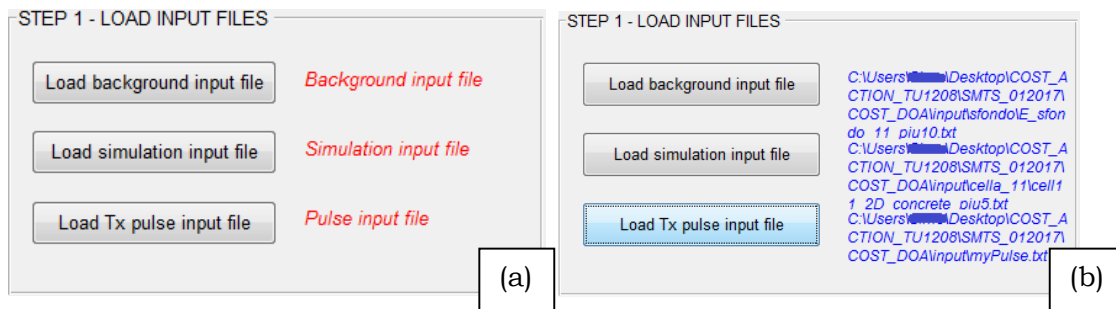


**FIG. 3** – Step 1: Load input files: a) Before selection and b) after the files have been selected.

### BACKGROUND INPUT FILE FORMAT (.TXT)

The SPOT-GPR tool is based on the two-dimensional geometry sketched in Fig. 1, where objects of arbitrary sections are embedded in a host medium. The background input file is a matrix of real values representing a collection of  $N$  traces that would be measured by the GPR in the absence of the targets ( $N$  has to be equal to the number of traces included in the radargram that the user wants to process).

The background input file can be produced by using an electromagnetic simulator, else it can be built from experimental data (the user can select in the B-scan a few traces measured in an area where, for sure, no targets are present; such traces can be averaged and the resulting trace can be repeated  $N$  times, to build the background input file).



Let us assume that each trace composing the radargram is a vector of T real values. Then, the background input file is a matrix of  $T \times N$  real values. Such matrix has to be saved as a .txt file, formatted in the following way:

```
(v1,1)space(v1,2)space(v1,3)space(v1,3)space(v1,5)...space(v1,N)
(v2,1)space(v2,2)space(v2,3)space(v2,3)space(v2,5)...space(v2,N)
...
(vT,1)space(vT,2)space(vT,3)space(vT,3)space(vT,5)...space(vT,N)
```

Additional spaces (vertical or horizontal) or text are not allowed. An example of background input file is given in Figure 4.

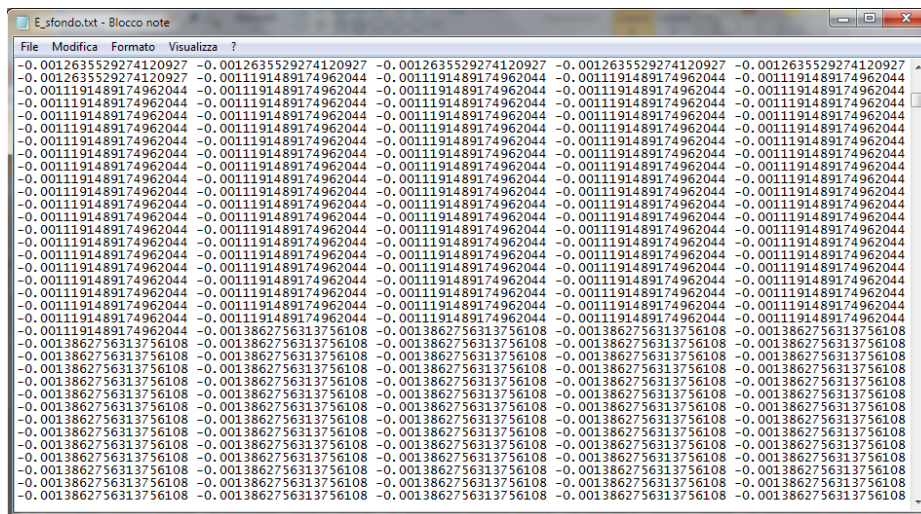


FIG. 4 – Background input file format – example.

### SIMULATION INPUT FILE FORMAT (.TXT)

The so-called simulation input file contains the synthetic or experimental radargram that the user is willing to process, with N traces. Each trace is a vector of T real values. Hence, the simulation input file is a matrix of  $T \times N$  real values. Such matrix has to be saved as a .txt file, formatted in the following way:

```
(v1,1)space(v1,2)space(v1,3)space(v1,3)space(v1,5)...space(v1,N)
(v2,1)space(v2,2)space(v2,3)space(v2,3)space(v2,5)...space(v2,N)
...
(vT,1)space(vT,2)space(vT,3)space(vT,3)space(vT,5)...space(vT,N)
```



(vT,1)space(vT,2)space(vT,3)space(vT,3)space(vT,5)...space(vT,N)

Additional spaces (vertical or horizontal) or text are not allowed.

### **PULSE INPUT FILE FORMAT (.TXT)**

The pulse input file contains a vector of T' samples of the pulse emitted by the GPR. The vector has to be saved as a .txt file, formatted in the following way:

(v1,1)space(v1,2)space(v1,3)space(v1,4)...space(v1,T)

Additional spaces (vertical or horizontal) or text are not allowed.

## **2.2. STEP 2: SETTINGS**

The “Step 2: SETTINGS” panel collects the experimental/simulation GPR settings that were used to generate the input files described in Subsection 2.1. This information is exploited by the SAP-DoA method to provide an estimation of the positions of the targets.

All the relevant settings are described and commented in Table 2.

When a setting parameter is correctly entered, the red-coloured text description abreast turns into the green message “Done” (Figure 5).

After all settings have been entered (and all the red-coloured descriptions turned into a column of green messages), the “START” button below the SETTINGS panel becomes active and the SAP-DoA procedure can be executed.

When the software is executed, the first outputs that appear on the GUI are the grey-scale map of the B-scan and the colour map of the FFT, on top of the main window.

The FFT plot is the collection of the Fourier transformation of all the compressed received pulses. Each trace is cross-correlated, in the time domain, with the Tx-pulse; the output signal (compressed pulse) is then FFT-transformed.

The SAP-DoA method takes more time to return the crossing pattern, which is finally displayed within the SPOTTING panel, as shown in Figure 6(a). The sharper the frequency resolution, the longer it takes. While the SAP-DoA procedure is running, some pop-up messages appear, providing information about the calculation progress status.

### 2.3. STEP 3: SPOTTING

The user can now select an area of interest in the SPOTTING panel, by dragging a rectangular region with the mouse. The coordinates of the four vertices of the selected region will appear on the GUI, along with the estimated position of the target within the selected region.

When all the red-coloured text descriptions have turned into the green message “Done” (see Figure 6(b)), the spotting (estimation) session is complete. A new spotting session can now be started, by pressing the “NEW SPOT” button, so that a new area of interest can be selected and the position of a new target can be estimated.

### 2.4. DEMO FILES

A few demo files are available for the user, which can be used to practice with the software. Each file is the .txt properly converted version of the output file obtained by running a gprMax simulation; the considered scenarios are the concrete cells with reinforcing elements studied in [1, 10]. In particular, radargrams for three different concrete cells are given:

1. **cell\_11** folder: contains the .txt files for Cell 1.1 (original cell [10] and enlarged cells [1]).
2. **cell\_12** folder: contains the .txt files for Cell 1.2 (original cell [10] and enlarged cells [1]).
3. **cell\_13** folder: contains the .txt files for Cell 1.3 (original cell [10] and enlarged cells).

Additionally:

4. The **background** folder contains the .txt files of the background (gprMax results calculated without targets).
5. **MyPulse.txt**: .txt file of the pulse used for gprMax calculations.

The main settings to be used at Step 2 (see Subsection 2.3) are listed in Table 3.

The geometrical configuration and physical properties of Cells 1.1 and 1.2 are described in [1, 10]; SPOT-GPR results obtained for those cells are found in [1]. Here, we deal with Cell 1.3. The user is encouraged to try and reproduce the results presented in [1] and here, before using SPOT-GPR for the analysis of his/her own data.

**TABLE 2 – SETTINGS.**

<b>SETTING NAME (Unit)</b>	<b>DEMO FILES DESCRIPTION AND COMMENTS</b>
Centre frequency (MHz)	<b>Description:</b> Pulse centre frequency $f_c$ transmitted by the GPR (Tx pulse). <b>Comments:</b> We call this quantity: $f_c$ .
Bandwidth (MHz)	<b>Description:</b> Bandwidth of the Tx pulse. <b>Comments:</b> $[f_c - BB/2; f_c + BB/2]$ . We suggest considering a -10 dB bandwidth.
Frequency resolution (MHz)	<b>Description:</b> Frequency step to be used by the SAP-DoA procedure. For each frequency, the SAP-DoA procedure will estimate DoAs and triangulate them, thus producing a collection of crossings. <b>Comments:</b> For each point within the range $f_c - BB/2; f_{RES}; f_c + BB/2$ , the procedure is executed. The crossing patterns are summed up: the global crossing pattern is the sum of the patterns obtained at each frequency.
Time sampling (ns)	<b>Description:</b> Tx/Rx time sampling. <b>Comments:</b> Assumed the same in Tx and Rx.
Scan spatial sampling (m)	<b>Description:</b> Distance between consecutive A-scan traces. <b>Comments:</b> Ideally this is the spacing of a linear uniform array collecting all the A-scans simultaneously. As in GPR applications the scenario does not change with time, the A-scans can be collected in different instants.
Antenna-ground distance (m)	<b>Description:</b> Distance between Tx/Rx antennas and the interface between air and the material hosting the targets. <b>Comments:</b> Assumed same for Tx and Rx antennas.
Dielectric constant of ground (N/A)	<b>Description:</b> Relative permittivity of ground. <b>Comments:</b> In release 1.0, this is a real value, i.e., losses are not considered by the SAP-DoA procedure.
False-alarm probability (N/A)	<b>Description:</b> False alarm probability used by the SAP-DoA procedure for the crossing pattern filtering. <b>Comments:</b> Typically between $10^{-3}$ and $10^{-6}$ , depending on $f_{RES}$ . For a coarse $f_{RES}$ , a lower number of crossings has to be expected and a lower false-alarm probability is recommended.

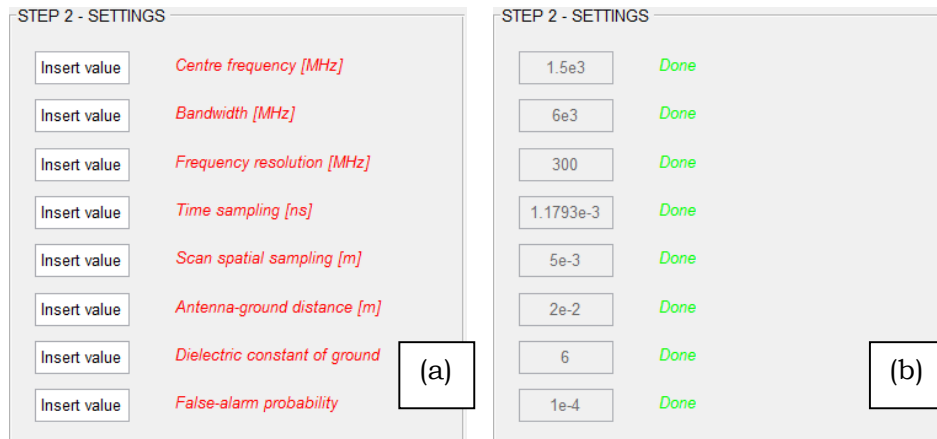


**FIG. 5** – Step 2: Settings: (a) Before entering the settings and (b) after all settings have been entered (release 1.0).

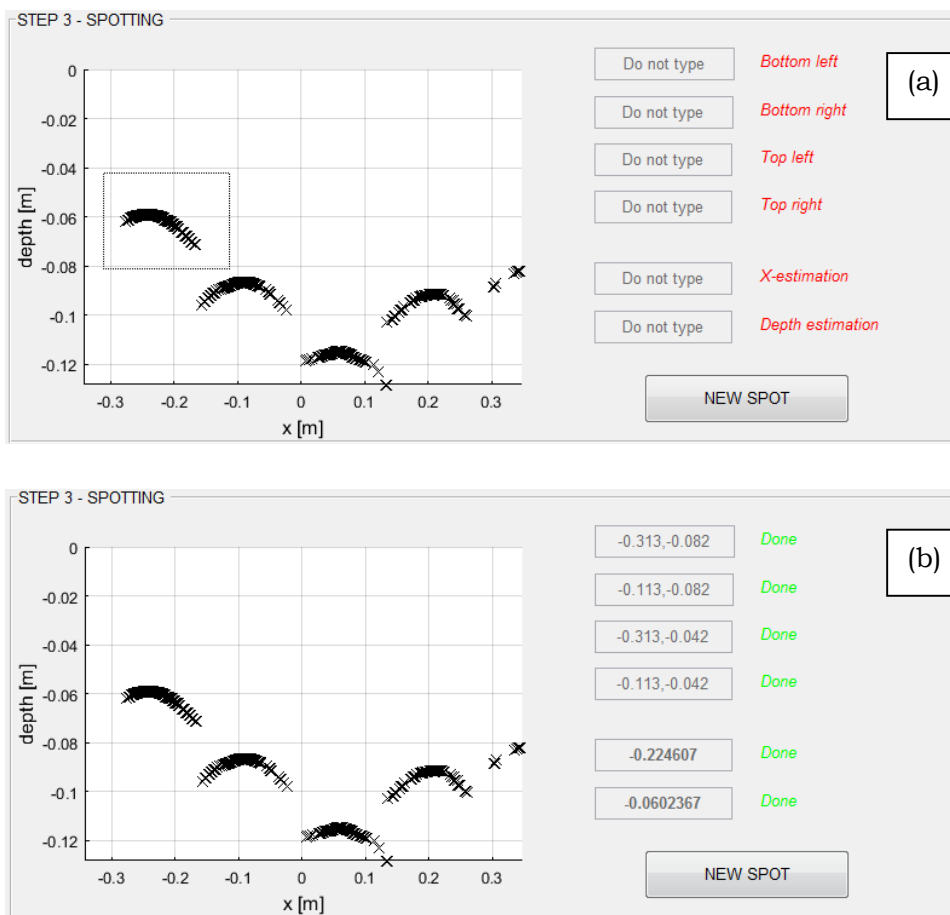


**FIG. 6** – Step 3: Spotting: (a) SAP-DoA procedure output and (b) target position estimation (release 1.0).

Table 4 resumes the physical and geometrical properties of Cell 1.3, which transverse section is schematized in Figure 7; the Table describes also four enlarged versions of the same structure. The cell hosts three metallic L-, □-, and U-shaped reinforcing elements and is positioned on a compacted fill. The original structure has a section of 60 × 18 cm; in this case, the reinforcing elements are rather close to each other and strong electromagnetic interactions take place when they are illuminated by a pulse emitted by a GPR; for this reason, although the geometry of the cell is rather simple, an accurate localization of the targets from GPR data is not a trivial task. We simulated four additional configurations, where we gradually increased the spacing between adjacent reinforcing elements with a 5-cm step, to investigate the performance of SPOT-GPR in the presence of different levels of interaction between targets.

**TABLE 3 – MAIN SETTINGS FOR ALL DEMO FILES.**

NAME	UNIT	VALUE
Center frequency	MHz	1.5E3
Bandwidth	MHz	6E3
Frequency resolution	MHz	300
Time sampling	ns	1.1793E-3
Scan spatial sampling	m	5E-3
Antenna-ground distance	m	2E-2
Dielectric constant of ground	N/A	6
False-alarm probability	N/A	1E-3 to 1E-6

In all the simulations, the central frequency of the pulse emitted by the GPR was  $f_c = 1.5$  GHz. The transmitting antenna (a dipole) and the receiving antenna (not modelled) were at 2 cm from the air-concrete interface; the distance between the antennas was 10 cm. Results were calculated on a time window of 5 ns, by moving the antennas along a line orthogonal to the axes of the targets. The distance between consecutive traces was 5 mm and the time sampling respected the Courant stability condition. The relative permittivity of concrete was  $\epsilon_{r,c} = 6$  and its conductivity was  $\sigma_c = 0.01$  S/m (but, SPOT-GPR 1.0 does not take into account the effects of losses in the host medium). The

relative permittivity of the compacted fill was  $\epsilon_{r,cf} = 16$  and its conductivity was  $\sigma_{cf} = 0.005$  S/m.

Figure 8 shows the radargram obtained for the original version of Cell 1.3, Figure 9 shows the radargrams for the enlarged versions of the cell. SPOT-GPR results are reported in Table 5, for the five considered configurations. For this cell, a hyperbolic fitting estimation would not yield good localization results, due to the shape and size of the targets: hyperbolic signatures in radargrams are generated by small circular-section targets. SPOT-GPR, instead, is capable to provide a rather accurate estimation of the positions of the targets; this result is considered to be significant, because it shows that our SAP-DoA approach can be successfully employed to detect objects different than cables, pipes and tubes.

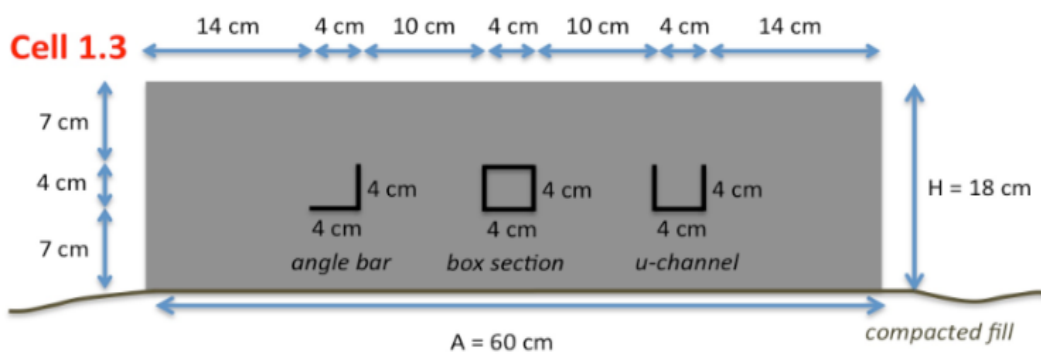


**FIG. 7** – Geometry of Cell 1.3 [10].

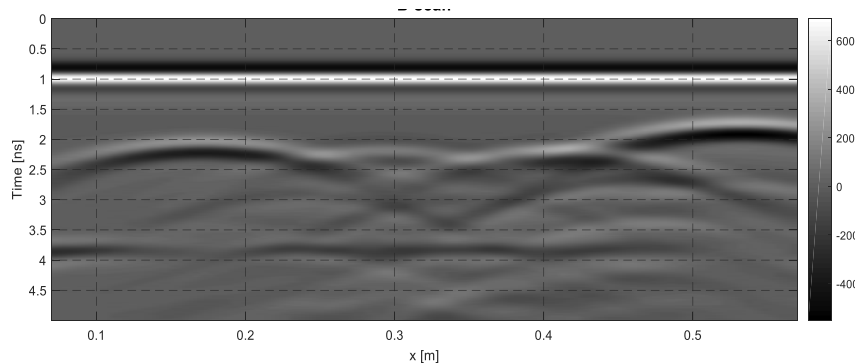


**FIG. 8** – Radargram for Cell 1.3 [10].



**TABLE 4 – CELL 1.3 SCENARIO (PEC STANDS FOR PERFECTLY CONDUCTING).**

<b>CELL 1-3 original</b>			
<b>Object</b>	<b>Position [m]</b>	<b>Shape</b>	<b>Material</b>
No. 1: Left	X: from 0.17 to 0.21 Y: from 0.12 to 0.16	L	Pec
No. 2: Centre	X: from 0.31 to 0.35 Y: from 0.12 to 0.16	□	Pec
No. 3: Right	X: From 0.45 to 0.49 Y: From 0.12 to 0.16	U	pec
<b>Cell section size: 0.60 x 0.28 cm<sup>2</sup> – Number of traces in the radargram: 100</b>			
<b>CELL 1-3 a)</b>			
<b>Object</b>	<b>Position [m]</b>	<b>Shape</b>	<b>Material</b>
No. 1: Left edge	X: from 0.17 to 0.21 Y: from 0.12 to 0.16	L	pec
No. 2: Centre	X: from 0.36 to 0.4 Y: from 0.12 to 0.16	□	pec
No. 3: Right edge	X: From 0.55 to 0.59 Y: From 0.12 to 0.16	U	pec
<b>Cell section size: 0.70 x 0.28 cm<sup>2</sup> – Number of traces in the radargram: 120</b>			
<b>CELL 1-3 b)</b>			
<b>Object</b>	<b>Position [m]</b>	<b>Shape</b>	<b>Material</b>
No. 1: Left	X: from 0.17 to 0.21 Y: from 0.12 to 0.16	L	pec
No. 2: Centre	X: from 0.41 to 0.45 Y: from 0.12 to 0.16	□	pec
No. 3: Right	X: From 0.65 to 0.69 Y: From 0.12 to 0.16	U	pec
<b>Cell section size: 0.80 x 0.28 cm<sup>2</sup> – Number of traces in the radargram: 140</b>			
<b>CELL 1-3 c)</b>			
<b>Object</b>	<b>Centre position [m]</b>	<b>Shape</b>	<b>Material</b>
No. 1: Left	X: from 0.17 to 0.21 Y: from 0.12 to 0.16	L	pec
No. 2: Centre	X: from 0.46 to 0.5 Y: from 0.12 to 0.16	□	pec
No. 3: Right	X: From 0.75 to 0.79 Y: From 0.12 to 0.16	U	pec
<b>Cell section size: 0.96 x 0.28 cm<sup>2</sup> – Number of traces in the radargram: 160</b>			
<b>CELL 1-3 d)</b>			
<b>Object</b>	<b>Centre position [m]</b>	<b>Radius [m]</b>	<b>Material</b>
No. 1: Left edge	X: from 0.17 to 0.21 Y: from 0.12 to 0.16	N/A shape: L	pec
No. 2: Centre	X: from 0.51 to 0.55 Y: from 0.12 to 0.16	N/A shape: □	pec
No. 3: Right edge	X: From 0.85 to 0.89 Y: From 0.12 to 0.16	N/A shape: U	pec
<b>Cell dimensions: 1.06 x 0.28 cm<sup>2</sup> – Number of traces in the radargram: 180</b>			
<b>Relative permittivity medium 1: 6 (concrete)</b>			
<b>Relative permittivity medium 2: 16 (compacted fill)</b>			
<b>Trace spacing: 5 cm - Time window: 5 ns - Centre freq: 1500 MHz (Ricker pulse)</b>			

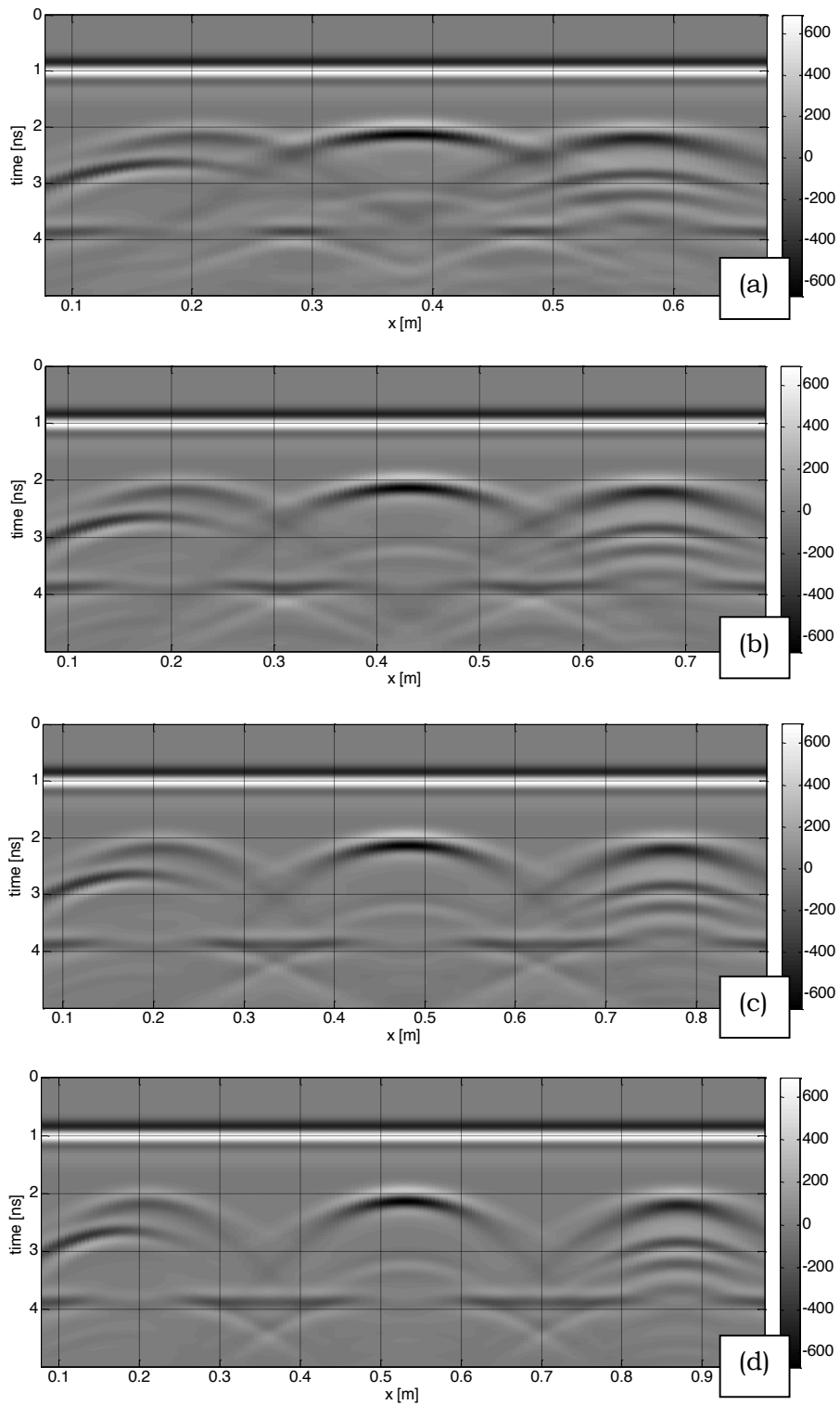


**FIG. 9** – Radargrams for enlarged versions of Cell 1.3. The distance between adjacent targets is increased of (a) 5 cm, (b) 10 cm, (c) 15 cm, and (d) 20 cm.

**TABLE 5 – SPOT-GPR RESULTS FOR CELL 1.3: POSITION ERROR.**

<b>CELL 1-3 original</b>	
<b>Object</b>	<b>SAP-DOA position error [m]</b>
No. 1: Left	(0.00001, -0.008)
No. 2: Centre	(-0.005, 0.008)
No. 3: Right	(0.0026, 0.008)
<b>CELL 1-3 a)</b>	
<b>Object</b>	<b>SAP-DOA position error [m]</b>
No. 1: Left	(0.001, 0.008)
No. 2: Centre	(-0.0005, 0.008)
No. 3: Right	(0.0033, 0.008)
<b>CELL 1-3 b)</b>	
<b>Object</b>	<b>SAP-DOA position error [m]</b>
No. 1: Left	(-0.013, 0.008)
No. 2: Centre	(-0.00425, 0.008)
No. 3: Right	(-0.001, 0.008)
<b>CELL 1-3 c)</b>	
<b>Object</b>	<b>SAP-DOA position error [m]</b>
No. 1: Left	(-0.01, 0.008)
No. 2: Centre	(-0.0014, 0.008)
No. 3: Right	(0.00001, 0.008)
<b>CELL 1-3 d)</b>	
<b>Object</b>	<b>SAP-DOA position error [m]</b>
No. 1: Left	(-0.01, 0.008)
No. 2: Centre	(0.0018, 0.008)
No. 3: Right	(0.003, 0.008)

### 3. CONCLUSIONS

In this paper, practical information was given on how to use SPOT-GPR release 1.0, a freeware tool implementing a Sub-Array Processing (SAP) approach. The tool has a graphical user interface; it can be employed to analyse Ground-Penetrating Radar (GPR) data and estimate the position of targets in a two-dimensional scenario.

The implemented procedure is based on beamforming techniques widely used in radar systems different than GPR, consisting in the estimation of the Direction of Arrival (DoA) of the incoming signals, in order to decipher how many scatterers are present and predict their positions.

So far, SPOT-GPR was tested only on synthetic radargrams generated by using gprMax; in the near future, we plan to test our software on experimental data, as well (in particular, we will use the TU1208

dataset coming from measurements performed at the IFSTTAR Geophysical Test Site, in Nantes, France).

In release 1.0 of SPOT-GPR, only the MULTiple Signal Classification (MUSIC) DoA algorithm is available; however, many other algorithms exist and can be easily implemented, such as the high-resolution approach Estimation of Signal Parameters via Rotational Invariance Technique (ESPRIT) [2]. Based on our preliminary investigations, MUSIC and ESPRIT are the most efficient DoA algorithms, for the purposes of analysing GPR radargrams. However, we already implemented and tested also the Bartlett, Capon, Linear Prediction, Maximum Entropy, Minimum Norm, and Pisarenko Harmonic Decomposition approaches. Because some users might be interested in comparing the performance of different algorithms on particular scenarios, we will release a new version of SPOT-GPR soon, where all these algorithms will be available.

Our plans for future work also include: the publication of results obtained by comparing SPOT-GPR with an automatic detection algorithm based on neural networks developed at the Faculty of Technical Sciences of Novi Sad (Serbia) [7]-[9]; and the integration of our SAP-DoA approach with Support-Vector-Machine techniques, in cooperation with the University of Genoa (Italy) [11]. The latter techniques are expected to increase the robustness of our approach with respect to the distance between sought targets, as they are considered to be more powerful than standard DoA algorithms in handling electromagnetic interactions between objects.

#### **4. ACKNOWLEDGEMENT**

The tool described in this paper was developed during three Short-Term Scientific Missions funded by COST and is a contribution to the COST Action TU1208 “Civil engineering applications of Ground Penetrating Radar.” The authors are grateful to COST for funding and supporting the Action TU1208.

#### **REFERENCES**

- [1] S. Meschino and L. Pajewski, “SPOT-GPR: A Freeware Tool for Target Detection and Localization in GPR Data Developed within the COST Action

TU1208,” *Journal of Telecommunications and Information Technology*, 2017, vol. 3, pp.43-54.

[2] S. Chandran, *Advances in Direction-of-Arrival Estimation*. Norwood, MA: Artech House, 2005.

[3] R. Kumaresan and D. W. Tufts, “Estimating the angles of arrival of multiple plane waves,” *IEEE Transactions on Aerospace and Electronic Systems*, vol. 19, no. 1, pp. 13–139, 1983.

[4] C. E. Cook and M. Bernfeld, *Radar Signals: An Introduction to Theory and Application*, 1st ed. Artech House Radar Library, 1993.

[5] C. Warren, A. Giannopoulos, and I. Giannakis, “gprMax: Open source software to simulate electromagnetic wave propagation for Ground Penetrating Radar,” *Computer Physics Communications*, vol. 209, pp. 163–170, 2016.

[6] Bello. Y. Idi and Md. N. Kamarudin, “Utility mapping with Ground Penetrating Radar: an innovative approach,” *Journal of American Science*, vol. 7, no. 1, pp. 644–649, 2011.

[7] A. Ristić, Ž. Bugarinović, M. Vrtunski, M. Govedarica and D. Petrovački, Integration of modern remote sensing technologies for faster utility mapping and data extraction, *Construction and Building Materials*, vol. 154, pp. 1183-1198, 2017.

[8] A. Ristic, Z. Bugarinovic, M. Govedarica, L. Pajewski, and X. Derobert, “Verification of Algorithm for Point Extraction from Hyperbolic Reflections in GPR Data,” 9th International Workshop on Advanced Ground Penetrating Radar, 28-30 June 2017, Nantes, France, pp. 1-5.

[9] A. Ristic, M. Vrtunski, M. Govedarica, L. Pajewski, and X. Derobert, “Automated Data Extraction from Synthetic and Real Radargrams of District Heating Pipelines,” 9th International Workshop on Advanced Ground Penetrating Radar, 28-30 June 2017, Nantes, France, pp. 1-5.

[10] L. Pajewski, A. Giannopoulos, “Electromagnetic modelling of Ground Penetrating Radar responses to complex targets,” *Short Term Scientific Missions and Training Schools – Year 1, COST Action TU1208*, L. Pajewski & M. Marciniak, Eds., Aracne Editrice, Rome, Italy, May 2014, ISBN 978-88-548-7225-7, pp. 7-45.

[11] M. Pastorino and A. Randazzo, "A smart antenna system for direction of arrival estimation based on a support vector regression," in *IEEE Transactions on Antennas and Propagation*, vol. 53, no. 7, pp. 2161-2168, July 2005.